

Consistent Energy-Based Atomistic/Continuum Coupling for Two-Body Potential: 1D and 2D Case

Alexander V. Shapeev*

May 4, 2022

Abstract

This paper concerns the problem of consistent energy-based coupling of atomistic and continuum models of materials, limited to zero-temperature statics of simple crystalline materials. It has been widely recognized that the most practical coupled methods exhibit finite errors on the atomistic/continuum interface (which are often attributed to spurious forces called “ghost forces”). There are only few existing works that propose a coupling which is sufficiently accurate near the interface under certain limitations. In this paper a novel coupling that is free from “ghost forces” is proposed for a two-body interaction potential under the assumptions of either (i) one spatial dimension, or (ii) two spatial dimensions and piecewise affine finite elements for describing the continuum deformation. The computational efficiency of the proposed coupling is demonstrated with numerical experiments. The coupling strategy is based on judiciously defining the contributions of the atomistic bonds to the discrete and the continuum potential energy. The same method in one dimension has been independently developed and analyzed by Li and Luskin (2010).

Keywords: atomistic model, consistent atomistic/continuum coupling, ghost force removal, atomistic bond contribution, multiscale method, finite element method

AMS subject classification: 65N30, 70C20, 74G15, 74G65

1 Introduction

In many applications of solid mechanics, such as modeling cracks, structural defects, or nano-electromechanical systems (NEMS), the classical continuum description is not suitable, and it is required to utilize an atomistic description of materials. However, full atomistic simulations are prohibitively expensive, hence there is a need for efficient numerical methods that couple a continuum description of a material in the region where material deformation is smooth and an atomistic description where the deformation gradient is large.

All methods of atomistic/continuum coupling can be divided into two categories: the energy-based coupling and the force-based coupling. The energy-based coupling [3, 13, 14, 17, 25, 33, 35, 36] consists in composing the energy of the system depending on both discrete and continuum deformations, and driving the system to a stable equilibrium. The underlying energy formulation

*Section of Mathematics, Swiss Federal Institute of Technology (EPFL), Station 8, CH-1015, Lausanne, Switzerland (alexander@shapeev.com).

of the energy-based coupled methods results in a number of advantages, for instance, one can apply an efficient nonlinear conjugate gradient solver [24] to it, or more easily formulate adaptive algorithms based on a posteriori error estimates [1, 27]. The essential disadvantage of the energy-based atomistic/continuum coupling is the presence of interfacial errors (which are often attributed to spurious forces called “ghost forces” [28]), which persistently arise in any practical coupled method [4, 24]. Due to this, the energy-based methods are usually less accurate than the force-based methods. Nevertheless, it has been observed in a recent benchmark [24] that introducing a ghost-force correction could make the energy-based methods as accurate as the force-based methods, although ghost-force correction requires extra computational effort.

In one dimension the problem of consistent zero-temperature static energy-based coupling is easy to solve [13, 22, 25]. However in higher dimensions this is a true challenge. In the case of nearest neighbor interaction there are methods that are free from ghost forces (the Coupling of Length Scales method [3] is an example of such a method), but in a general situation all methods of coupling introduce a certain interfacial error.

Several methods have been proposed to address the problem of consistent energy-based coupling, including the quasinonlocal (QNL) quasicontinuum method [31] and the geometrically consistent scheme (GCS) [13, 25] which may be regarded as a generalization of QNL. The latter method consists in two steps: first, passing from the general finite range interaction to the nearest neighbor interaction in the padding region between the atomistic and continuum region, and second, passing from the nearest neighbor atomistic model to the continuum model. E, Lu, and Yang proved that the latter method exhibits no ghost forces in 1D and no ghost forces in 2D and 3D in the case of a straight (planar) interface which is aligned with the lattice and contains no corners [13].

Another noteworthy effort to minimize the ghost forces is a work of Klein and Zimmerman [17] who considered a problem of coupling for arbitrarily overlapping atomistic and continuum regions. Assuming a two-body interatomic potential, they proposed a method to compute the contributions of the atomistic bonds in the overlapping region by numerically minimizing the ghost forces using the least squares technique.

In the force-based methods [15, 18, 19, 23, 28, 30], the equilibrium is achieved by computing the generalized forces for each degree of freedom (associated with the atoms and the finite element nodes) and driving them to zero. Most of such methods exhibit no ghost forces by construction, but pose other sort of difficulties arising from the force field being nonconservative [10, 11, 24].

Recently there has appeared a number of analytical works studying energy-based and force-based coupling, most of the works assume a 1D second nearest neighbor interaction setting. The inconsistent energy-based coupling has shown to exhibit large errors whereas the consistent QNL coupling and a more general GCS method (for finite-range interactions) are uniformly accurate [7, 25, 26]. The studies of accuracy and stability of coupled methods near critical deformations (i.e., when the system is about to become unstable) show that an inconsistent coupling significantly under-predicts the critical strain, whereas the consistent QNL coupling remains accurate up to the critical strain [7, 8]. The ghost-force correction to energy-based methods has shown to incorrectly predict the atomistic instabilities if the parameters for correction iterations are not chosen carefully [6]. Furthermore, it has been shown that iterative correction of ghost forces for energy-based methods gives effectively the same result as force-based methods [5].

For the force-based methods (namely, the 1D force-based quasicontinuum method, QCF) Dobson, Luskin, and Ortner showed that the respective QCF operator is not positive definite and therefore the usual stability criterion does not apply to QCF [10]. They have also formulated the

stability criterion in terms of eigenvalues (dynamic stability) and showed that QCF is dynamically stable up to critical strains. In a later work [9] they have proposed to apply the GMRES method to QCF. Analysis shows that it can be an efficient and reliable solver for QCF [9, 12].

Thus, from the above review of existing works we conclude that consistent energy-based atomistic/continuum coupling could be an ideal method for modeling atomistic statics, however applicability of existing energy-based coupled methods is very limited. The popular alternative is the consistent force-based coupling, however more work is needed to fully address the difficulties arising from non-positive definiteness of the force-based coupling.

In the present paper a new energy-based atomistic/continuum coupling is proposed, which does not suffer from ghost forces. The coupling is based on judiciously treating the atomic bonds crossing the atomistic/continuum interface, proportionally splitting their contributions between discrete and continuum energy. The way of splitting the contributions of the energy was drawn from ideas of the projection method described in [22]. Two variants of the method are formulated, the first couples the atomistic and the continuum energies through the atoms inside the continuum region and the second performs coupling only through the interface. The scope of the present paper is limited to a two-body interaction potential, one or two spatial dimensions, and piecewise linear finite element discretization of the continuum deformation (the latter assumption is only for the 2D case). No restrictions on the finite element mesh (except that its nodes are positioned at the lattice sites) are made.

We note that the same method in one-dimensional setting has been independently proposed and analyzed by Li and Luskin [21].

The paper is organized as follows: Section 2 introduces the problem of atomistic/continuum coupling and briefly discusses major difficulties. In Section 3 the proposed methods are presented in detail in a 1D setting and then extended to a two-dimensional case in Section 4. The numerical experiments illustrating performance of the proposed methods are presented in Section 5. The paper ends with a discussion of the results (Section 6) and concluding remarks (Section 7).

2 Atomistic/Continuum Coupling in 1D

In order to give a more vivid illustration of the proposed methods, we will start with a 1D problem formulation followed by a detailed presentation of the proposed methods in 1D (Section 3). We will then show how to extend the proposed methods to two dimensions in Section 4.

2.1 Atomistic Model

Consider a 1D atomistic material described by positions of atoms in the reference configuration as $x_i = i$ ($i \in \mathbb{Z}$). For simplicity we set the lattice parameter $\epsilon = 1$. Let \mathcal{I} be a set of indices of atoms present in the atomistic material. Atoms may displace from their reference positions x_i to positions y_i and their displacements are $u_i = y_i - x_i$. The generic linear space containing x_i , y_i , and u_i will be denoted as $\mathcal{U} = \{g : \mathcal{I} \rightarrow \mathbb{R}\}$. For elements of \mathcal{U} introduce the forward difference operator D_r as follows:

$$(D_r g)_i = D_r g_i = \frac{g_{i+r} - g_i}{r}.$$

Note that if $i + r \notin \mathcal{I}$ then $D_r g_i$ is undefined, therefore, strictly speaking, D_r should not be considered as an operator $\mathcal{U} \rightarrow \mathcal{U}$.

The interaction of the atoms is described by the potential φ and the cut-off radius R , yielding the total interaction energy

$$E(y) = \sum_{\substack{i,j \in \mathcal{I} \\ 1 \leq j-i \leq R}} \varphi(y_j - y_i) = \sum_{\substack{i,i+r \in \mathcal{I} \\ 1 \leq r \leq R}} \varphi(rD_r y_i). \quad (1)$$

In practice, the proximity of atoms is measured in the physical domain, i.e., the atoms i and j contribute a non-zero interaction energy if $|y_j - y_i| \leq \tilde{R}$. However, for the purpose of studying consistency of the method, this treatment is essentially the same as $|j - i| \leq R$, since they are equivalent on the uniform deformation $y_i = Fx_i$.

We consider the Dirichlet-type boundary conditions, namely we fix the positions y_i of atoms $i \in \mathcal{I}_D$ near the boundary:

$$y_i = Fx_i \quad (i \in \mathcal{I}_D), \quad (2)$$

where F is an arbitrary deformation tensor. To avoid boundary effects, we require that every unconstrained atom i has a full set of neighbors:

$$(\forall i \in \mathcal{I} \setminus \mathcal{I}_D) (\forall r \in \mathbb{Z} : |r| \leq R) \quad i+r \in \mathcal{I}. \quad (3)$$

The boundary conditions span a manifold of admissible deformations and the linear space of test functions

$$\mathcal{U}_D = \{y \in \mathcal{U} : y_i = Fx_i \ (\forall i \in \mathcal{I}_D)\}, \quad \mathcal{U}_0 = \{u \in \mathcal{U} : u_i = 0 \ (\forall i \in \mathcal{I}_D)\}.$$

Under the assumption (3), elements of \mathcal{U}_0 satisfy

$$\sum_{i,i+r \in \mathcal{I}} D_r v_i = 0 \quad (\forall v \in \mathcal{U}_0, \forall r \in \mathbb{Z} : 1 \leq |r| \leq R). \quad (4)$$

Compute the variation of $E(y)$:

$$E'(y; v) = \sum_{\substack{i,i+r \in \mathcal{I} \\ 1 \leq r \leq R}} \varphi'(rD_r y_i) r D_r v_i.$$

The equations of equilibrium of the atomistic material under the external force f_i in variational form can be written as

$$\text{find } y \in \mathcal{U}_D: \quad E'(y; v) = \sum_{i \in \mathcal{I}} f_i v_i \quad \forall v \in \mathcal{U}_0. \quad (5)$$

These equations admit the solution described by a uniform strain $y = Fx$, as is shown by the following computation:

$$E'(Fx; v) = \sum_{\substack{i,i+r \in \mathcal{I} \\ 1 \leq r \leq R}} \varphi'(rF) r D_r v_i = \sum_{1 \leq r \leq R} \varphi'(rF) r \left(\sum_{i,i+r \in \mathcal{I}} D_r v_i \right) = 0, \quad (\forall v \in \mathcal{U}_0) \quad (6)$$

which is due to (4).

The problem (5), although discrete, is usually too large to handle on a computer. Therefore, its approximations with reduced degrees of freedom are used. Normally, for a numerical method whose energy is $\tilde{E}(y)$ to converge, one must also have $\tilde{E}'(Fx; v) = 0 \ (\forall v \in \mathcal{U}_0)$. This relation is sometimes called the “*patch test*”, a term borrowed from the theory of finite elements to describe the necessary condition for nonconforming elements to converge [32].

2.2 Continuum Model

If the deformation gradient $y_{i+1} - y_i$ is smooth in a neighborhood of a certain domain Ω_c , the exact atomistic model (1) can be approximated with the continuum one

$$E_c(y) = \sum_{r=1}^R \int_{\Omega_c} \varphi(ry'(x))dx, \quad (7)$$

where $y \in W^{1,\infty}(\Omega_c)$ is a continuum approximation to the discrete deformation: $y_i \approx y(i)$. The formula (7) is essentially the Cauchy-Born rule [2], where we approximate the interaction energy using the energy density $\sum_{r=1}^R \varphi(ry'(x))$.

Compute the variation of the continuum energy:

$$E'_c(Fx, v) = \sum_{r=1}^R \int_{\Omega_c} \varphi(rF)rv'(x)dx = \left(\sum_{r=1}^R \varphi(rF)r \right) \int_{\Omega_c} v'(x)dx.$$

If the deformation at the boundary of the continuum region is fixed, i.e., the admissible deformations v satisfy $v|_{\partial\Omega_c} = 0$, then, as follows from application of the Green's formula to the above formula, the uniform strain $y(x) = Fx$ is also an equilibrium in the continuum model.

2.3 Problem Formulation

Consider an atomistic material which in its reference configuration occupies the region $\Omega = (-N - R, N + R)$. The material will be treated continuously in the *continuum region* $\Omega_c = (0, N)$ and discretely in the *atomistic region* $\Omega_a = \Omega \setminus \overline{\Omega_c}$ (here $\overline{\bullet}$ denotes the closure of a set), the atomistic/continuum interface is $\Gamma := \partial\Omega_c = \{0, N\}$. Define the atomistic lattice $\mathcal{I} = \Omega \cap \mathbb{Z}$, the atoms within the atomistic region $\mathcal{I}_a = \Omega_a \cap \mathbb{Z}$, and the set $\mathcal{I}_D = \{i \in \mathbb{Z} : N \leq |i| < N + R\}$ containing atoms involved in formulation of the Dirichlet-type boundary conditions (2). For these \mathcal{I} and \mathcal{I}_D , the relation (3) holds and hence (4) also holds.

Note that from algorithmic point of view, fixing the positions of atoms $i \geq N + 1$ (i.e., near the right boundary) is redundant, since for the continuum model in the region $(0, N)$ it is sufficient to fix the position only for the atom $i = N$. Nevertheless, to compare the approximate model with the fully atomistic one, it is convenient to keep these atoms fixed, as we will see below.

It should also be noted that the regions were chosen in this way only for ease of visualization, and the discussion below is valid for a more general family of regions Ω_a , Ω_c , and \mathcal{I}_D . After presenting and discussing the proposed methods in 1D, we will extend the method to the multidimensional case where we will assume a general form of the regions.

The deformation of the material will thus be defined on $\mathcal{I}_a \cup \Gamma \cup \Omega_c$:

$$\begin{aligned} \mathcal{U} &= \{y : \mathcal{I}_a \cup \Omega_c \rightarrow \mathbb{R} : y|_{\Omega_c} \in W^{1,\infty}(\Omega_c)\}, \\ \mathcal{U}_0 &= \{u \in \mathcal{U} : u_i = 0 \ (\forall i \in \mathcal{I}_D)\}. \end{aligned}$$

A typical element of \mathcal{U} is shown in Figure 1. Here and below we interchangeably use the notation $y_i = y(i) = y(x_i)$ for the values of $y \in \mathcal{U}$.

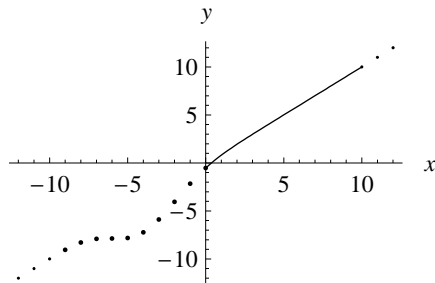


Figure 1: A typical element y of \mathcal{U} , $N = 10$, $R = 3$. The smaller points correspond to \mathcal{I}_D .

2.4 Example of Straightforward Coupling

The most straightforward approach to atomistic/continuum coupling consists in writing the atomistic energy in the form

$$E(y) = \sum_{i \in \mathcal{I}} \left(\frac{1}{2} \sum_{\substack{i+r \in \mathcal{I} \\ 1 \leq |r| \leq R}} \varphi(|r| D_r y_i) \right)$$

and interpreting the expression in the parentheses as the energy associated with a particular atom $i \in \mathcal{I}$. Then we can substitute the atomistic energy associated with atoms $i \notin \Omega_a$ in the expression (1) by the continuum energy:

$$E(y) \sim E^{\text{sc1}}(y) = \sum_{i \in \mathcal{I}_a} \left(\frac{1}{2} \sum_{\substack{i+r \in \mathcal{I} \\ 1 \leq |r| \leq R}} \varphi(|r| D_r y_i) \right) + E_c(y),$$

where $E_c(y)$ is defined in (7). Such a coupling results in the ghost forces. Indeed, even for the nearest neighbor interaction (i.e., for $R = 1$), one has

$$\begin{aligned} (E^{\text{sc1}})'(y; v) &= \sum_{i \in \mathcal{I}_a} \left(\frac{1}{2} \sum_{\substack{i+r \in \mathcal{I} \\ r = \pm 1}} \varphi'(F) D_r v_i \right) + E'_c(y; v) \\ &= \frac{1}{2} \varphi'(F) \sum_{i=-N+1}^{-1} (D_1 v_i + D_{-1} v_i) + \int_0^N \varphi'(F) v'(x) dx \\ &= \frac{1}{2} \varphi'(F) (v_0 + v_{-1}) + \varphi'(F) (0 - v(0)) = -\varphi'(F) \frac{v_0 - v_{-1}}{2}. \end{aligned}$$

In this case the reason for not getting a zero force is quite clear: it is because the bond $(-1, 0)$ adjacent to the interface Γ is not fully accounted for.

One can propose a method with more careful treatment of the interface Γ to include such bonds

into the energy:

$$E(y) \sim E^{\text{sc}2}(y) = \frac{1}{2} \sum_{1 \leq |r| \leq R} \left(\sum_{\substack{i \in \mathcal{I}_a \\ i+r \in \mathcal{I}}} \varphi(|r|D_r y_i) + \sum_{\substack{i \in \Gamma \\ i+r \in \mathcal{I}_a}} \varphi(|r|D_r y_i) \right) + E_c(y), \quad (8)$$

Here special treatment was applied to atoms on the interface Γ between the two regions: the bonds with atoms $i+r \in \mathcal{I}_a$ are treated atomistically, whereas the bonds with atoms $i+r \in \Omega_c$ are effectively treated continuously. Such a coupling, after discretization with piecewise linear elements, resembles the so-called energy-based quasicontinuum (QCE) method [33] or the Coupling of Length Scales (CLS) method [3].

The above coupling has no ghost forces for the nearest neighbor interaction. There is, however, a ghost force for second nearest neighbor interaction (i.e., when considering the terms with $r = 2$). Indeed, omitting the straightforward but tedious calculations, one can derive (for $R = 2$):

$$(E^{\text{sc}2})'(Fx, v) = \frac{1}{2} \varphi'(2F) (v_{-1} - 2v_0 + v_1 - v_{N-1}),$$

The interpretation of the nonzero force, for instance, on atom $i = -1$ can be as follows. The interaction of atoms $i = -1$ and $i = 1$ is computed two times in a different manner: once according to the continuum strain $2y'(x_1)$ and once according to the exact strain $y_1 - y_{-1}$. The first computation contributes the force fully to the continuum region, which causes loss of balance of forces on the atom $i = -1$.

A possible approach to removing the ghost forces is to further modify the energy $E^{\text{sc}2}(y)$ in such a way that the uniform deformation $y(x) = Fx$ is the solution to the equations. In the context of the quasicontinuum method, this was first done in [31] for the second nearest neighbor ($R = 2$) and then generalized in [13, 25] to longer interactions. However, when generalizing the methods from dimension one to higher dimensions, additional difficulties arise, for instance related to transition between so-called element-based and atom-based summation rules [13]. In particular, presence of faces that are not aligned with the lattice or interface corners (interface edges and vertices in 3D) results in ghost forces.

2.5 On the Projection Method

The consistent coupling that will be proposed in this paper is closely related to the ideas of the projection method described in [22]. The projection method assumes piecewise affine interpolation of deformation in the continuum region, but avoids forming the Cauchy-Born energy density assuming the exact atomistic interaction everywhere. Due to this, the projection method is naturally free from the ghost forces.

Let us formally split the exact atomistic energy (1) into the energy of the bonds within the atomistic region ($E_1(y)$), the bonds within the continuum region ($E_2(y)$), and the bonds crossing the interface Γ ($E_3(y)$):

$$\begin{aligned} E(y) &= \sum_{\substack{i, i+r \in \mathcal{I}_a \cup \Gamma \\ 1 \leq r \leq R}} \varphi(rD_r y_i) + \sum_{\substack{i, i+r \in \mathcal{I}_c \cup \Gamma \\ 1 \leq r \leq R}} \varphi(rD_r y_i) + \sum_{\substack{i \in \mathcal{I}_a \\ i+r \in \mathcal{I}_c \\ 1 \leq r \leq R}} \varphi(rD_r y_i) \\ &=: E_1(y) + E_2(y) + E_3(y). \end{aligned}$$

Note that in this formal splitting we ignored the contribution of the bonds near the boundaries of Ω .

For a moment assume that the deformation in the continuum region $\Omega_c = (0, N)$ is affine, i.e., that $y'(x) = \frac{y_N - y_0}{N} =: y'_c \forall x \in \Omega_c$, and substitute it into E_2 :

$$E_2(y) = \sum_{\substack{i, i+r \in [0, N] \cap \mathbb{Z} \\ 1 \leq r \leq R}} \varphi(ry'_c) = \sum_{r=1}^R (N+1-r) \varphi(ry'_c) = E_c(y) - \sum_{r=1}^R (r-1) \varphi(ry'_c). \quad (9)$$

This identity can be interpreted as follows: $E_2(y)$ contains the energy of all the bonds within Ω_c , which coincides with $E_c(y)$ up to a correction $\sum_{r=1}^R (r-1) \varphi(ry'_c)$. This correction is needed since we accounted for the bonds that are partly within Ω_c in $E_3(y)$. The ideas of correction of continuum energy to minimize ghost forces have been used in [17].

In the next section we will propose a way of carefully accounting for the energy of atomic bonds, which will enable us to formulate a truly consistent atomistic/continuum coupling.

3 The Proposed Consistent Atomistic/Continuum Coupling in One Dimension

We propose a strategy of constructing a consistent coupling between the atomistic and the continuum models. The strategy is based on splitting the energy associated with each atomic bond into atomistic and continuum contributions.

The first proposed method of consistent coupling is based on combining the *exact and the continuum contributions* of the bonds (hereinafter referred to as the ECC method).

3.1 Method of Combining Exact and Continuum Contributions

Introduce some preliminary terms and definitions. The term *bond* between atoms i and $i+r$ will refer to an open interval $b = (i, i+r)$. Introduce the set of all bonds in the atomistic system

$$\mathcal{B} := \{(i, i+r) : 1 \leq r \leq R, i \in \mathcal{I}, i+r \in \mathcal{I}\}.$$

We denote the potential energy of the bond $b = (i, i+r)$ as

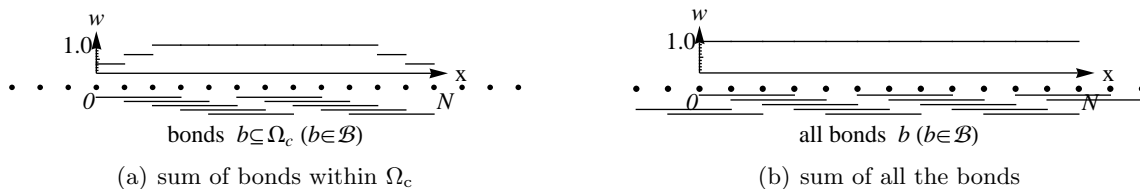
$$e_{(i, i+r)}(y) := \varphi(rD_r y_i) \quad (10)$$

and call it the *exact contribution* of the bond $(i, i+r)$ to the potential energy. Thus, the exact atomistic potential energy (1) can be written as

$$E(y) = \sum_{b \in \mathcal{B}} e_b(y). \quad (11)$$

For a bond $b = (i, i+r) \subset \Omega_c$ we define its contribution to the continuum energy, or, in short, *continuum contribution*, as

$$c_b(y) := \frac{1}{r} \int_b \varphi \left(r \frac{\partial y}{\partial x} \right) dx \quad (\text{if } b \subset \Omega_c).$$


 Figure 2: Illustration of (16) and (17), $N = 12$, $r = 3$.

Compute its variation on the uniform deformation $y = Fx$ and compare with the variation of the exact contribution:

$$c'_{(i,i+r)}(Fx; v) = \frac{1}{r} \int_{x_i}^{x_{i+r}} \varphi'(rF) r \frac{\partial v}{\partial x} dx = \varphi'(rF) v|_{x_i}^{x_{i+r}} = \varphi'(rF)(v_{i+r} - v_i), \quad (12)$$

$$e'_{(i,i+r)}(Fx; v) = \varphi'(rF) r D_r v_i = \varphi'(rF)(v_{i+r} - v_i). \quad (13)$$

It can be seen that the variation of the exact contribution $e_b(y)$ and the continuum contribution $c_b(y)$ coincide. This means that in construction of a numerical method, $e_b(y)$ can be substituted with $c_b(y)$.

Following this idea, substitute $e_b(y)$ with $c_b(y)$ in (11) for the bonds fully contained in the continuum region:

$$E(y) \approx E^{\text{ecc}}(y) := \sum_{\substack{b \in \mathcal{B} \\ b \not\subset \Omega_c}} e_b(y) + \sum_{\substack{b \in \mathcal{B} \\ b \subset \Omega_c}} c_b(y) =: E_a^{\text{ecc}}(y) + E_c^{\text{ecc}}(y). \quad (14)$$

The calculations (12)–(13) and (6) immediately prove the consistency of $E^{\text{ecc}}(y)$:

$$(E^{\text{ecc}})'(Fx; v) = \sum_{\substack{b \in \mathcal{B} \\ b \not\subset \Omega_c}} e'_b(Fx; v) + \sum_{\substack{b \in \mathcal{B} \\ b \subset \Omega_c}} c'_b(Fx; v) = \sum_{b \in \mathcal{B}} e'_b(Fx; v) = E'(Fx; v) = 0.$$

The rest of this subsection will be devoted to showing that $E^{\text{ecc}}(y)$ can be computed efficiently, i.e., without a need to go through all the bonds $b \in \Omega_c$. Simplify the continuum contributions:

$$E_c^{\text{ecc}}(y) = \sum_{\substack{b \in \mathcal{B} \\ b \subset \Omega_c}} c_b(y) = \sum_{\substack{b \in \mathcal{B} \\ b \subset \Omega_c}} \frac{1}{r} \int_{\Omega_c} \chi_b(x) \varphi(ry'(x)) dx = \int_{\Omega_c} \left(\sum_{\substack{b \in \mathcal{B} \\ b \subset \Omega_c}} \frac{\chi_b(x)}{r} \right) \varphi(ry'(x)) dx \quad (15)$$

where χ_\bullet is the characteristic function of a region. The sum of characteristic functions in the parentheses can be computed explicitly as

$$w(x) = \left(\sum_{\substack{b \in \mathcal{B} \\ b \subset \Omega_c}} \frac{\chi_b(x)}{r} \right)_{\text{a.e.}} = \min \left(1, \frac{1}{r} [\text{dist}(x, \Omega_a)] \right), \quad (16)$$

where $\lceil \bullet \rceil$ is the ceiling function. (Note that this equality should be understood as “equals almost everywhere”.) As can be seen, well inside Ω_c (i.e., for $\text{dist}(x, \Omega_a) > r$) we recover exactly the continuum energy (7). This is because any point x in Ω_c (except, of course, the lattice positions $x \in \mathbb{Z}$) is covered by exactly r bonds of the form $b = (i, i + r) \in \mathcal{B}$ (see illustration of the function $w(x)$ in Figure 2(a)). The reason we do not recover the complete continuum energy is that the bonds crossing the interface (and thus not being contained fully in Ω_c) are computed in a fully discrete manner. In the next subsection we will propose a method whose continuum energy is exactly (7).

In view of the above discussion, we can verify, as long as (3) holds, that

$$\frac{1}{r} \sum_{b \in \mathcal{B}} \chi_b(x) \Big|_{x \in \Omega_c} = 1, \quad (17)$$

see illustration in Figure 2(b). Hence if we define the continuum contribution of an arbitrary bond $b = (i, i + r)$ as

$$c_b(y) := \frac{1}{r} \int_{\Omega_c \cap b} \varphi \left(r \frac{\partial y}{\partial x} \right) dx \quad (18)$$

and compute the continuum contribution of all the bonds in the system, we will get exactly the continuum energy of Ω_c :

$$\begin{aligned} \sum_{b \in \mathcal{B}} c_b(y) &= \sum_{b \in \mathcal{B}} \frac{1}{r} \int_{\Omega_c \cap b} \varphi(ry'(x)) dx = \sum_{b \in \mathcal{B}} \frac{1}{r} \int_{\Omega_c} \chi_b(x) \varphi(ry'(x)) dx \\ &= \int_{\Omega_c} \varphi(ry'(x)) dx = E_c(y). \end{aligned} \quad (19)$$

Therefore we can write (cf. (15)):

$$E_c^{\text{ecc}}(y) = \sum_{\substack{b \in \mathcal{B} \\ b \subset \Omega_c}} c_b(y) = E_c(y) - \sum_{\substack{b \in \mathcal{B} \\ b \not\subset \Omega_c}} c_b(y),$$

which is, remarkably, very similar to the analog of continuum energy $E_2(y)$ in the projection method (9). This expression of continuum energy is also related to ideas of Klein and Zimmerman of correcting the Cauchy-Born energy in the finite elements near the interface Γ [17].

Thus, we rewrite (14) as

$$E^{\text{ecc}}(y) = \sum_{\substack{b \in \mathcal{B} \\ b \not\subset \Omega_c}} (e_b(y) - c_b(y)) + E_c(y).$$

According to this formula, assembling the energy can be done as follows: we go through all the atoms in the atomistic region, computing the energy of their interaction with all other atoms and subtracting continuum contribution of the energy (18) (of course, if $\Omega_c \cap b$ is nonempty). Seen in this way, the method can be implemented efficiently, performing a single loop over the atoms within the atomistic region only.

3.2 Method of Combining Atomistic and Continuum Contributions

The method proposed in the previous subsection consists in treating each bond that does not fully lie in the continuum region atomistically and modifying the continuum energy by subtracting the corresponding contribution from the continuum energy. Since the positions of atoms which are strictly inside Ω_c enter the expression of the total energy, the coupling between regions becomes nonlocal. For implementation it may be more preferable to have a coupling through the interface only. In this subsection we show how to accomplish it.

The calculation (19) indicates that the method with the exact continuum energy $E_c(y)$ should contain all the continuum contributions $c_b(y)$. Then we should derive an “atomistic contribution” $a_{(i,i+r)}(y)$ which would consistently balance $c_{(i,i+r)}(y)$.

To do that, define the operator $D_\omega y$ for $\omega \subset \Omega$ ($\omega \neq \emptyset$) in the following way. If $\omega = \bigcup_{m=1}^M (l_m, r_m)$ is a union of non-intersecting intervals then

$$D_\omega y := \frac{1}{|\omega|} \sum_{m=1}^M (y(r_m) - y(l_m)),$$

where $|\omega|$ is the total length of ω . $D_\omega y$ has the following properties:

1. $D_\omega y$ approximates the derivative of y , in particular $D_\omega(Fx) = F$.
2. $D_{(i,i+r)}y = D_r y_i$.
3. If $\omega = \omega_1 \cup \omega_2$ and $\omega_1 \cap \omega_2 = \emptyset$ then $|\omega|D_\omega y = |\omega_1|D_{\omega_1}y + |\omega_2|D_{\omega_2}y$.
4. $\int_\omega v'(x)dx = |\omega|D_\omega v$.

Using this operator define the *atomistic contribution* of a bond $b = (i, i + r)$ as

$$a_b(y) := \frac{|b \cap \Omega_a|}{r} \varphi(r D_{b \cap \Omega_a} y). \quad (20)$$

Compute the variations of the atomistic and the continuum (cf. (18)) contributions of a bond $(i, i + r) = b \in \mathcal{B}$, using the properties 4 and 1 of D_ω :

$$\begin{aligned} c'_b(Fx; v) &= \frac{1}{r} \int_{b \cap \Omega_c} \varphi'(rF) r \frac{dv}{dx} dx = \varphi'(rF) |b \cap \Omega_c| D_{b \cap \Omega_c} v, \quad \text{and} \\ a'_b(Fx; v) &= \frac{|b \cap \Omega_a|}{r} (\varphi'(rF) r D_{\Omega_a \cap b} v) = \varphi'(rF) |b \cap \Omega_a| D_{b \cap \Omega_a} v, \end{aligned} \quad (21)$$

and therefore, using the properties 3 and 2 of D_ω , one can see that

$$c'_b(Fx; v) + a'_b(Fx; v) = \varphi'(rF) |b| D_b v = \varphi'(rF) D_r v_i = e'_b(Fx; v).$$

This immediately implies that if we define the energy

$$E^{\text{acc}}(y) := \sum_{b \in \mathcal{B}} a_b(y) + \sum_{b \in \mathcal{B}} c_b(y) =: E_a^{\text{acc}}(y) + E_c^{\text{acc}}(y)$$

then the coupling given by $E^{\text{acc}}(y)$ is consistent:

$$(E^{\text{acc}})'(Fx; v) = \sum_{b \in \mathcal{B}} e'_b(Fx; v) = E'(Fx; v) = 0.$$

We will call it the *atomistic and continuum contributions* method (ACC in short).

Due to (19) the method can be written as

$$E^{\text{acc}}(y) = \sum_{b \in \mathcal{B}} a_b(y) + E_c(y). \quad (22)$$

Note that in (22) the sum over $b \in \mathcal{B}$ can be effectively changed to the sum over $(b \in \mathcal{B}, b \not\subset \Omega_c)$, since if $b \subset \Omega_c$ then $a_b(y) = 0$.

The prominent feature of the method is that the atomistic part of the energy can be seen to depend only on the deformation in the atomistic region and on the interface. This is more convenient for implementation (see Section 4.5) and can potentially help in parallelization of the method.

We conclude this discussion by presenting another version of atomistic contribution $a_b(y)$. If $b \cap \Omega_c$ is a union of non-intersecting intervals (ξ_m, η_m) ($1 \leq m \leq M$) then we define

$$\tilde{a}_b(y) := \sum_{m=1}^M \frac{\eta_m - \xi_m}{r} \varphi \left(r \frac{y_{\eta_m} - y_{\xi_m}}{\eta_m - \xi_m} \right).$$

Its variation

$$\tilde{a}'_b(Fx; v) = \sum_{m=1}^M \frac{\eta_m - \xi_m}{r} \varphi'(rF) r \frac{v_{\eta_m} - v_{\xi_m}}{\eta_m - \xi_m} = \varphi'(rF) \sum_{m=1}^M (v_{\eta_m} - v_{\xi_m})$$

coincides with the variation $a'_b(Fx; v)$ (cf. (21)) and hence $a_b(y)$ can be substituted by $\tilde{a}_b(y)$ in the approximation (22):

$$\tilde{E}^{\text{acc}}(y) = \sum_{b \in \mathcal{B}} \tilde{a}_b(y) + E_c(y).$$

The approximation $\tilde{E}^{\text{acc}}(y)$ has a potentially smaller number of coupled terms when the bonds cross the interface several times (this is more likely to happen in many dimensions) which may be easier for implementation. In the present work the ACC method was implemented for the convex atomistic/continuum interface, in which case both methods coincide.

3.3 Summary and Formulation of the Proposed Methods in One Dimension

The key component of derivation of the ECC and ACC methods is the identity (17), which somewhat resembles partition of unity. This identity led to representation of the continuum energy as a sum of contribution of all the bonds (19).

To formulate the method we define a *bond* as an interval between the interacting atoms: $b = (i, i + r)$. The bond's *exact* $e_b(y)$, *continuous* $c_b(y)$, and *atomistic* $a_b(y)$ *contributions* are defined

by formulae (10), (18), and (20) respectively. Then the two proposed methods read

$$E^{\text{ecc}}(y) = \sum_{\substack{b \in \mathcal{B} \\ b \notin \Omega_c}} (e_b(y) - c_b(y)) + E_c(y), \quad \text{and}$$

$$E^{\text{acc}}(y) = \sum_{\substack{b \in \mathcal{B} \\ b \notin \Omega_c}} a_b(y) + E_c(y).$$

Both methods are consistent (i.e., ghost-force-free) by construction and can be implemented efficiently, that is, by performing effectively a single loop over atoms in the atomistic region.

The energy of the ECC method is closer to the exact atomistic energy $E(y)$, but on the other hand its formulation involves nonlocal coupling of atomistic and continuum regions. The ACC method, on the contrary, approximates the contribution of more bonds, but the coupling between the atomistic and the continuum region is done only through the interface Γ .

We note that the same coupling has been independently proposed and analyzed by Li and Luskin in a one-dimensional discrete setting. In [21] they introduce an extension of the QNL method [31] to the finite-range potential (i.e., arbitrary R), which is essentially equivalent to the ECC method of the present work, and analyze it in a linearized discrete setting without coarsening (that is, for functions $y(x)$ which are piecewise affine on each interval $i-1 \leq x \leq i$, $i = 1, 2, \dots, N$). In particular, they prove that (i) under certain assumptions the uniform deformation is a stable equilibrium, and (ii) the coupled method converges to the exact atomistic solution.

In order to extend the method to two dimensions, in the next section we derive a two-dimensional analog of partition of unity (17), based on which we define the continuum contributions, and then define the atomistic contributions so that the variation of the continuum plus the atomistic contributions gives the variation of the exact contribution.

4 Atomistic/Continuum Coupling in Two Dimensions

Coupling of atomistic and continuum models of materials becomes harder in many dimensions. For instance, the quasinonlocal quasicontinuum method [31] and its generalizations [13, 25] suffer from ghost forces if the atomistic/continuum interface has corners or faces which are not aligned with the lattice.

In this section we will extend the ECC and ACC methods to two dimensions. The methods will be consistent by construction, with no restrictions on the mesh (except that its nodes coincide with lattice sites).

In the two-dimensional case the reference configuration is usually described by a uniform lattice $x_i = Ai$ (where $i \in \mathbb{Z}^2$, $x_i \in \mathbb{R}^2$, $A \in \mathbb{R}^{2 \times 2}$), and the deformed configuration y_i is often considered as given by some mapping $Y : \mathbb{R}^2 \rightarrow \mathbb{R}^2$. However, in our analysis we will adopt a slightly different point of view where we set $x_i = i$ and the uniform deformation tensor A will be accounted for as $y_i = Y(Ax_i)$ (this is done, for instance, in [20]). This point of view is actually closer to computer implementation, where the lattice is indexed with integers, rather than real numbers. We stress that this is not a limitation of the proposed methods; in fact the numerical examples (Section 5) will be presented for a hexagonal crystal with $A = \begin{pmatrix} 1 & -1/2 \\ 0 & \sqrt{3}/2 \end{pmatrix}$.

4.1 Preliminaries

4.1.1 Regions and Triangulation

Consider an open bounded region $\Omega \subset \mathbb{R}^2$, the atomistic and the continuum regions $\Omega_a \subset \Omega$, $\Omega_c = \Omega \setminus \overline{\Omega_a}$ (also open), the atomistic/continuum interface $\Gamma = \partial\Omega_c$. We also consider the atomistic lattice $\mathcal{I} = \Omega \cap \mathbb{Z}^2$, the atoms within the atomistic region $\mathcal{I}_a = \Omega_a \cap \mathbb{Z}^2$, and the set of atoms involved in posing the Dirichlet-type boundary conditions $\mathcal{I}_D \subset \mathcal{I} \cap \overline{\Omega_a}$. To avoid boundary effects, we will make additional assumptions on \mathcal{I} and \mathcal{I}_D after we introduce atomistic interaction (in Section 4.1.3).

We further assume that Ω_c is a polygon with vertices coinciding with some lattice locations x_i . We will perform the fully discrete analysis, hence we introduce a triangulation \mathcal{T} of Ω_c with triangles $T \in \mathcal{T}$ whose vertices are also positioned at the lattice locations x_i . The space of continuous piecewise affine finite elements on Ω_c is denoted as $\mathcal{P}_1(\mathcal{T})$. This setting is exactly the same as the one of the QC method [33]. However, the difference between the QC and the proposed methods will be in the way the atomistic and continuum energies are coupled.

4.1.2 Operators

Introduce the discrete differentiation:

$$(D_r y)_i = D_r y_i = \frac{y_{i+r} - y_i}{|r|}.$$

Define an interval (x_1, x_2) between two points $x_1, x_2 \in \mathbb{R}^2$ as a set

$$(x_1, x_2) := \{(1 - \lambda)x_1 + \lambda x_2 : \lambda \in (0, 1)\}.$$

Define integrals over such intervals as:

$$\int_{(x_1, x_2)} f(x) db := |x_2 - x_1| \int_0^1 f((1 - \lambda)x_1 + \lambda x_2) d\lambda.$$

The following property then holds:

$$\int_{(x_1, x_2)} \frac{\partial f}{\partial r} db = f(x_2) - f(x_1),$$

where the directional derivative is defined as

$$\frac{\partial f}{\partial r} := \frac{r}{|r|} \cdot \nabla f.$$

4.1.3 Atomistic Model and Continuum Approximation

We assume that atomistic interaction is given by a set of neighbors $\mathcal{R} \subset \mathbb{Z}^2 \setminus \{0\}$ and a two-body potential φ . Denote the collection of all bonds in the system as

$$\mathcal{B} := \{(i, i + r) : r \in \mathcal{R}, i \in \mathcal{I}, i + r \in \mathcal{I}\}.$$

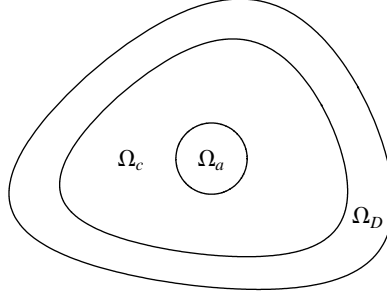


Figure 3: Illustration of a possible choice of the regions Ω_a , Ω_c , and Ω_D . If Ω_D is “thick” enough than (26) and (27) are satisfied with $\mathcal{I}_D = \Omega_D \cap \mathbb{Z}^2$.

and the *exact contribution* of a bond $b = (i, i + r) \in \mathcal{B}$ under the deformation y as

$$e_b(y) = \varphi(|r| |D_r y_i|). \quad (23)$$

It should be understood that r and i here essentially depends on b , but to simplify the notations we will avoid writing r_b or i_b .

The energy of the atomistic model then reads

$$E(y) = \sum_{b \in \mathcal{B}} e_b(y), \quad (24)$$

and its continuum approximation based on the Cauchy-Born rule can be written as

$$E_c(y) = \int_{\Omega_c} \sum_{r \in \mathcal{R}} \varphi \left(|r| \left| \frac{dy}{dr} \right| \right) d\Omega. \quad (25)$$

To avoid boundary effects entering our analysis, similarly to the 1D assumption (3), we assume

$$(\forall i \in \mathcal{I} \setminus \mathcal{I}_D) (\forall r \in \mathcal{R}) \quad i + r \in \mathcal{I}, \quad \text{and} \quad (26)$$

$$(\forall r \in \mathcal{R}) (\forall i \in \mathbb{Z}^2 : (i, i + r) \cap \overline{\Omega_c} \neq \emptyset) \quad i, i + r \in \mathcal{I}. \quad (27)$$

Practically, these assumptions mean that we have enough atoms \mathcal{I}_D whose position we fix so that each free atom near the boundary of Ω (and hence of $\Omega_c \subset \Omega$) has enough neighbors to interact. It can be achieved by choosing a region Ω_D near the boundary of Ω , such that $\Omega_D \cap \Omega_c = \emptyset$ and

$$\text{dist}(\Omega \setminus \Omega_D, \partial\Omega) > \max_{r \in \mathcal{R}} |r|$$

(see illustration on Figure 3). Then $\mathcal{I}_D = \Omega_D \cap \mathbb{Z}^2$ will satisfy (26) and (27).

One can now show that the uniform deformation $y = Fx$ is an equilibrium of the atomistic energy (24). Indeed, compute

$$e'_{(i, i+r)}(Fx; v) = \frac{\varphi'(|Fr|)}{|Fr|} Fr \cdot |r| D_r v_i. \quad (28)$$

Then notice that for $v \in \mathcal{U}_0$ and $r \in \mathcal{R}$

$$\sum_{i, i+r \in \mathcal{I}} D_r v_i = 0$$

due to the assumption (26). Finally compute

$$E'(Fx; v) = \sum_{(i, i+r) \in \mathcal{B}} |r| \frac{\varphi'(|Fr|)}{|Fr|} Fr \cdot D_r v_i = \sum_{r \in \mathcal{R}} |r| \frac{\varphi'(|Fr|)}{|Fr|} Fr \cdot \sum_{i, i+r \in \mathcal{I}} D_r v_i = 0.$$

Below we propose two consistent coupling, i.e., methods whose variation on the uniform deformation $y = Fx$ is also zero. These methods of coupling are generalizations of the one-dimensional ECC and ACC couplings (cf. (14) and (22) respectively).

4.1.4 Analog of Partition of Unity

Our first aim in construction of a consistent method in \mathbb{R}^2 is to obtain the 2D analog of the partition of unity in 1D case (17). There is a number of difficulties to overcome in the \mathbb{R}^2 case. First difficulty is that the bonds, defined essentially as 1D objects, cannot add up to 1 in a 2D region Ω_c , which means that we have to look for weaker analogs of (17). The other difficulty is that geometrically some bonds may be positioned on the interface between two triangles in 2D, in which case we should split its contribution equally between the triangles. However, the interface of a triangle is a set of zero area, hence standard $W^{1,\infty}$ -functions do not have well-defined values there.

To address the second difficulty, we define the characteristic function for a set $\omega \subset \mathbb{R}^2$ in the following way:

$$\chi_\omega(x) = \lim_{\rho \rightarrow 0} \frac{|\omega \cap B_\rho(x)|}{|B_\rho(x)|},$$

where $B_\rho(x)$ is the ball with radius ρ and center x , and $|\bullet|$ is the measure of the set. We will only consider polygonal regions ω , for which (i) the limit w.r.t. $\rho \rightarrow 0$ in the definition of $\chi_\omega(x)$ exists, and (ii) including/excluding the boundary of ω (or any part of it) does not change the values of $\chi_\omega(x)$. These assumptions are always true for polygonal regions (which were used in all the practical 2D applications known to the author).

The characteristic function $\chi_\omega(x)$ for a triangle ω can be visualized as follows:

$$\chi_\omega(x) = \begin{cases} 1 & \text{if } x \in \text{interior of } \omega \\ \frac{1}{2} & \text{if } x \in \text{edge of } \omega \\ \frac{\alpha}{2\pi} & \text{if } x \text{ is a vertex of } \omega \text{ with angle } \alpha \\ 0 & \text{otherwise.} \end{cases} \quad (29)$$

Note that for the formulation of the method the values of $\chi_\omega(x)$ at the vertices of ω will not be important. For the characteristic function $\chi_\omega(x)$ thus defined, we have

$$\chi_{\Omega_c}(x) = \sum_{T \in \mathcal{T}} \chi_T(x), \quad (30)$$

where the identity is strictly pointwise (i.e., not just almost everywhere). It will now suffice to obtain an analog of partition of unity for a single triangle T . The following lemma prepares us to formulate a partition of unity for a single triangle T .

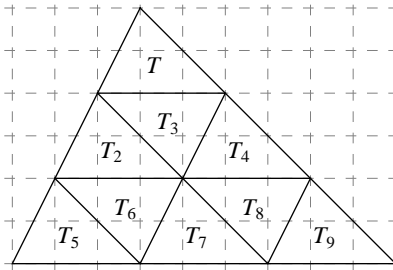


Figure 4: Illustration of the induction step of a proof that the triangle $3T$ can be partitioned with nine copies of T . We have a partition of $2T$ with triangles T, T_2, T_3, T_4 and we complete it to a partition of $3T$ by adding two parallelograms ($T_5 \cup T_6$ and $T_7 \cup T_8$) and one corner triangle T_9 .

Lemma 1 (Bond-Density Lemma). *Let T be a triangle in \mathbb{R}^2 whose vertices belong to the lattice \mathbb{Z}^2 . Then for any $r \in \mathbb{Z}^2$, $r \neq 0$ the following identity holds:*

$$\frac{1}{|r|} \sum_{i \in \mathbb{Z}^2} \int_{(i, i+r)} \chi_T(x) db = |T|. \quad (31)$$

Proof. Notice that if (31) is valid for triangles T_1 and T_2 ($T_1 \cap T_2 = \emptyset$), then it is valid for $T_1 \cup T_2$. Also notice that both sides of (31) are invariant w.r.t. translation of T by a vector $s \in \mathbb{Z}^2$ and reflection around a point $p \in \mathbb{Z}^2$. Using these transformations, we can obtain mT (a triangle obtained from stretching T by a factor $m \in \mathbb{Z}$) as a union of m^2 copies of T shifted by different vectors and possibly reflected. It can be proved by induction: for $m = 1$ the statement is trivial. Assuming that we have a partition of mT by m^2 copies of T , we can complete it to a partition of $(m + 1)T$ by placing m parallelograms (each of which consists of two triangles) next to a side of mT and one additional triangle at the corner of that side (see Figure 4 for illustration). Thus, we can partition $(m + 1)T$ by $m^2 + 2m + 1 = (m + 1)^2$ triangles.

Hence one has

$$\begin{aligned} \frac{1}{|r|} \sum_{i \in \mathbb{Z}^2} \int_{(i, i+r)} \chi_T(x) db &= \frac{1}{|r|m^2} \sum_{i \in \mathbb{Z}^2} \int_{(i, i+r)} \chi_{mT}(x) db \\ &= \frac{1}{|r|m^2} \left(\sum_{\substack{i \in \mathbb{Z}^2 \\ (i, i+r) \subset mT}} \int_{(i, i+r)} \chi_{mT}(x) db + O(m) \right) \\ &= \frac{1}{|r|m^2} \left(\sum_{\substack{i \in \mathbb{Z}^2 \\ (i, i+r) \subset mT}} |(i, i+r)| + O(m) \right) \\ &= \frac{1}{m^2} \left(\sum_{\substack{i \in \mathbb{Z}^2 \\ (i, i+r) \subset mT}} 1 + O(m) \right) \end{aligned}$$

$$= \frac{1}{m^2} (|mT| + O(m)) = |T| + O(m^{-1}).$$

Here the $O(m)$ terms appear first from neglecting contributions of the bonds near the boundary of mT (whose measure grows as $O(m)$) and then from estimating the number of points i for which $(i, i+r) \subset mT$ by $|mT|$, again making the error proportional to the measure of the boundary of mT . Letting $m \rightarrow \infty$ finally proves (31). \square

Remark 1. *Unfortunately, the 3D analog of lemma 1 is not true. One can take a bond direction $r = (1, 0, 0)$ and consider a tetrahedron T with vertices $(1, 0, 0)$, $(0, 1, 0)$, $(0, 0, 1)$, $(0, 1, 1)$. Then for each bond $(i, i+r)$ the left-hand side of (31) will be zero, although the right-hand side of (31) is $1/6$.*

As a corollary, we formulate a 2D analog of partition of unity, which will be the key to extending the proposed methods to two dimensions.

Lemma 2. *Let $r \in \mathbb{Z}^2$, $r \neq 0$, $y \in \mathcal{P}_1(\mathcal{T})$, and f be a continuous function $\mathbb{R}^2 \rightarrow \mathbb{R}$. Then the following identity holds:*

$$\frac{1}{|r|} \sum_{i, i+r \in \mathbb{Z}^2} \int_{(i, i+r)} \chi_{\Omega_c}(x) f\left(\frac{\partial y}{\partial r}\right) db = \int_{\Omega_c} f\left(\frac{\partial y}{\partial r}\right) d\Omega. \quad (32)$$

Proof. The proof is based on Lemma 1 and identity (30). Notice that $\frac{\partial y}{\partial r}$ is constant on each triangle. The following formal computation proves (32):

$$\begin{aligned} \frac{1}{|r|} \sum_{i, i+r \in \mathbb{Z}^2} \int_{(i, i+r)} \chi_{\Omega_c}(x) f\left(\frac{\partial y}{\partial r}\right) db &= \frac{1}{|r|} \sum_{i, i+r \in \mathbb{Z}^2} \int_{(i, i+r)} \sum_{T \in \mathcal{T}} \chi_T(x) f\left(\frac{\partial y}{\partial r}\right) db \\ &= \sum_{T \in \mathcal{T}} f\left(\frac{\partial y}{\partial r}\right) \Big|_T \left(\frac{1}{|r|} \sum_{i, i+r \in \mathbb{Z}^2} \int_{(i, i+r)} \chi_T(x) db \right) \\ &= \sum_{T \in \mathcal{T}} f\left(\frac{\partial y}{\partial r}\right) \Big|_T |T| = \int_{\Omega_c} f\left(\frac{\partial y}{\partial r}\right) d\Omega. \end{aligned} \quad (33)$$

To conclude the proof it remains to notice that the integral $\int_{(i, i+r)} \chi_T(x) f\left(\frac{\partial y}{\partial r}\right) db$ is defined when $(i, i+r) \cap \partial T \neq \emptyset$, i.e., when the interval $(i, i+r)$ partly or fully lies on a face F of T . In this case the vector r is parallel to F . Therefore, since $y \in \mathcal{P}_1(\mathcal{T})$ is continuous on F , its tangential derivative $\frac{\partial y}{\partial r}$ is also continuous on F , and hence $f\left(\frac{\partial y}{\partial r}\right)$ is a well-defined continuous function on F . Hence the formal calculation (33) is valid, which concludes the proof. \square

As a final step towards formulating the multidimensional analog of the proposed coupling, one can notice that due to the assumption (27), the sum in the left-hand of (32) can be changed to the sum over $(i, i+r) \in \mathcal{B}$, which immediately yields the following corollary.

Corollary 1. *Let $r \in \mathcal{R}$, $y \in \mathcal{P}_1(\mathcal{T})$, and f be a continuous function $\mathbb{R}^2 \rightarrow \mathbb{R}$. Then the following identity holds:*

$$\frac{1}{|r|} \sum_{(i, i+r) \in \mathcal{B}} \int_{(i, i+r)} \chi_{\Omega_c}(x) f\left(\frac{\partial y}{\partial r}\right) db = \int_{\Omega_c} f\left(\frac{\partial y}{\partial r}\right) d\Omega. \quad (34)$$

4.2 Method of Combining Exact and Continuum Contributions

In 2D the point values of $W^{1,\infty}$ -functions are not defined. Therefore, instead of coupling the atomistic model with the full continuum model, we consider coupling the atomistic model with the continuum model discretized with piecewise affine finite elements $\mathcal{P}_1(\mathcal{T})$. The deformations are then defined similarly to the 1D case:

$$\begin{aligned}\mathcal{U} &= \{y : \mathcal{I}_a \cup \overline{\Omega_c} \rightarrow \mathbb{R}^2 : y|_{\Omega_c} \in \mathcal{P}_1(\mathcal{T})\}, \\ \mathcal{U}_0 &= \{u \in \mathcal{U} : u_i = 0 \ (\forall i \in \mathcal{I}_D)\}.\end{aligned}$$

Having established the two-dimensional analog of partition of unity (Lemma 2 and Corollary 1), we can split the continuum energy into individual contributions. For that, apply Corollary 1 with the function $f(z) = \varphi(|r||z|)$ to the continuum energy (25):

$$\begin{aligned}E_c(y) &= \sum_{r \in \mathcal{R}_{\Omega_c}} \int \varphi\left(|r| \left| \frac{dy}{dr} \right| \right) d\Omega = \sum_{r \in \mathcal{R}} \frac{1}{|r|} \sum_{(i,i+r) \in \mathcal{B}_{(i,i+r)}} \int \chi_{\Omega_c}(x) \varphi\left(|r| \left| \frac{dy}{dr} \right| \right) db \\ &= \sum_{b \in \mathcal{B}} \frac{1}{|r|} \int_b \chi_{\Omega_c}(x) \varphi\left(|r| \left| \frac{dy}{dr} \right| \right) db,\end{aligned}$$

and define hence the *continuum contribution* of a bond $b \in \mathcal{B}$ as

$$c_b(y) := \frac{1}{|r|} \int_b \chi_{\Omega_c}(x) \varphi\left(|r| \left| \frac{dy}{dr} \right| \right) db. \quad (35)$$

Compute the variation of $c_{(i,i+r)}(y)$ for a bond $b = (i, i+r)$:

$$c'_b(Fx; v) = \frac{1}{|r|} \int_b \chi_{\Omega_c}(x) \frac{\varphi'(|Fr|)}{|Fr|} Fr \cdot |r| \frac{dv}{dr} db = \frac{\varphi'(|Fr|)}{|Fr|} Fr \cdot \int_b \chi_{\Omega_c}(x) \frac{dv}{dr} db. \quad (36)$$

Notice that if b is fully contained in the interior of Ω_c (i.e., $\chi_{\Omega_c}(x) = 1 \ \forall x \in b$) then the variation of $c_b(y)$ equals to the variation of $e_b(y)$ (cf. (28)).

Therefore, the atomistic/continuum coupling

$$E^{\text{ecc}}(y) := \sum_{\substack{b \in \mathcal{B} \\ b \not\subset \Omega_c}} e_b(y) + \sum_{\substack{b \in \mathcal{B} \\ b \subset \Omega_c}} c_b(y)$$

is consistent, i.e., $(E^{\text{ecc}})'(Fx; v) = 0 \ \forall v \in \mathcal{U}_0$. Remarkably, this formula is exactly the same as the 1D model (14) (although the respective objects are now in \mathbb{R}^2).

For implementation, the following expression of E^{ecc} is more convenient:

$$E^{\text{ecc}}(y) := \sum_{\substack{b \in \mathcal{B} \\ b \not\subset \Omega_c}} (e_b(y) - c_b(y)) + E_c(y). \quad (37)$$

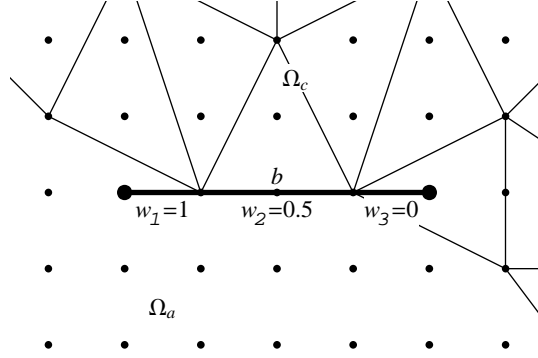


Figure 5: Illustration of splitting of a bond into several intervals in 2D. The bond b is split into three intervals, one with full contribution to the atomistic energy ($w_1 = 1$), the other with half contribution ($w_2 = 1/2$) and the third one with no contribution ($w_3 = 0$).

4.3 Method of Combining Atomistic and Continuum Contributions

We now define the atomistic contribution of a bond coherent with the continuum contribution (35). We start with expressing a bond $b = (i, i + r)$ as a union of non-intersecting intervals and points:

$$b = \left(\bigcup_{m=1}^M (\xi_m, \eta_m) \right) \cup \left(\bigcup_{l=1}^L \{\zeta_l\} \right),$$

so that

$$\chi_{\Omega_a} \Big|_{(\xi_m, \eta_m)} = w_m. \quad (38)$$

The illustration of splitting of a bond b into several intervals is shown in Figure 5. Then we define the *atomistic contribution*

$$a_b(y) = \frac{\sum_{m=1}^M w_m (\eta_m - \xi_m)}{|r|} \varphi \left(|r| \left| \frac{\sum_{m=1}^M w_m (y_{\eta_m} - y_{\xi_m})}{\sum_{m=1}^M w_m (\eta_m - \xi_m)} \right| \right). \quad (39)$$

Remark 2. *If the atomistic/continuum interface Γ is convex, then the expression for $a_b(y)$ can be greatly simplified, since in that case not more than one section of b can have a nonzero weight w_m and if the weight is not equal to one then this section of b lies on the interface Γ .*

Compute the variation of $a_b(y)$:

$$\begin{aligned} a'_b(Fx; v) &= \frac{\sum_{m=1}^M w_m (\eta_m - \xi_m)}{|r|} \frac{\varphi'(|Fr|)}{|Fr|} Fr \cdot |r| \frac{\sum_{m=1}^M w_m (v_{\eta_m} - v_{\xi_m})}{\sum_{m=1}^M w_m (\eta_m - \xi_m)} \\ &= \frac{\varphi'(|Fr|)}{|Fr|} Fr \cdot \sum_{m=1}^M w_m (v_{\eta_m} - v_{\xi_m}), \end{aligned}$$

compare it to (36):

$$\begin{aligned} c'_{(i,i+r)}(Fx; v) &= \frac{\varphi'(|Fr|)}{|Fr|} Fr \cdot \sum_{m=1}^M \int_{\xi_m}^{\eta_m} (1 - w_m) \frac{dv}{dr} db \\ &= \frac{\varphi'(|Fr|)}{|Fr|} Fr \cdot \sum_{m=1}^M (1 - w_m) (v(\eta_m) - v(\xi_m)), \end{aligned}$$

and observe that

$$a'_b(Fx; v) + c'_b(Fx; v) = e'_b(Fx; v).$$

Thus, the approximation

$$E^{\text{acc}}(y) := \sum_{b \in \mathcal{B}} a_b(y) + \sum_{b \in \mathcal{B}} c_b(y) = \sum_{\substack{b \in \mathcal{B} \\ b \notin \Omega_c}} a_b(y) + E_c(y) \quad (40)$$

is consistent.

Remark 3. *The choice of atomistic contribution (39) is not unique. One can, for instance, define*

$$\tilde{a}_b(y) = \sum_{m=1}^M \frac{w_m(\eta_m - \xi_m)}{|r|} \varphi \left(|r| \left| \frac{y_{\eta_m} - y_{\xi_m}}{\eta_m - \xi_m} \right| \right)$$

and notice that

$$\begin{aligned} \tilde{a}'_b(Fx; v) &= \sum_{m=1}^M \frac{w_m(\eta_m - \xi_m)}{|r|} \frac{\varphi'(|Fr|)}{|Fr|} Fr \cdot |r| \frac{v_{\eta_m} - v_{\xi_m}}{\eta_m - \xi_m} \\ &= \frac{\varphi'(|Fr|)}{|Fr|} Fr \cdot \sum_{m=1}^M w_m (v_{\eta_m} - v_{\xi_m}) = a'_b(Fx; v), \end{aligned}$$

which makes the following alternative version of (40),

$$\tilde{E}^{\text{acc}}(y) := \sum_{b \in \mathcal{B}} \tilde{a}_b(y) + \sum_{b \in \mathcal{B}} c_b(y) = \sum_{\substack{b \in \mathcal{B} \\ b \notin \Omega_c}} \tilde{a}_b(y) + E_c(y), \quad (41)$$

be consistent as well. However, in relation to Remark 2, one can show that the two methods will coincide in the case of the convex atomistic/continuum interface.

4.4 Summary of the Proposed Methods

We have proposed two versions of atomistic/continuum coupling that are free from ghost forces. The setting for the coupling is exactly the same as for the QC method: the continuum deformation is discretized with piecewise affine elements and the element nodes coincide with the lattice (see Section 4.1). The difference with the QC method consists in coupling the atomistic and continuum energies.

The formulation of the coupling involves definitions of

1. a *bond* $b = (i, i + r)$ between atoms i and $i + r$ (i and $i + r$ are positions of atoms in the reference configuration) as an interval of a straight line joining i and $i + r$, and
2. the *exact* $e_b(y)$, the *continuous* $c_b(y)$, and the *atomistic* $a_b(y)$ *contributions* of a bond b by formulae (23), (35), and (39) respectively.

The exact and continuum contributions (ECC) method is then defined as

$$E^{\text{ecc}}(y) := \sum_{\substack{b \in \mathcal{B} \\ b \not\subset \Omega_c}} (e_b(y) - c_b(y)) + E_c(y),$$

and the atomistic and continuum contributions (ACC) method is defined as

$$E^{\text{acc}}(y) := \sum_{\substack{b \in \mathcal{B} \\ b \not\subset \Omega_c}} a_b(y) + E_c(y),$$

where $E_c(y)$ is the continuum energy (25) which was defined according to the Cauchy-Born rule, \mathcal{B} is the set of all atomistic bonds in the system, and Ω_c is the continuum region.

4.5 Notes on Implementation

In this section we discuss some aspects of implementation of the ACC method (40) in 2D. Implementation of the ECC method (37) is in many ways similar, but one has to take extra efforts to compute the continuum contributions (35) for bonds crossing the interface, which may require to compute line integrals over several triangles $T \in \mathcal{T}$.

The ACC energy (40) can be thought of a sum of continuum energy $E_c(y)$, and the respective atomistic contributions over the bonds which are not fully inside Ω_c (i.e., bonds that are inside Ω_a or crossing the interface Γ). The continuum energy is treated using finite elements: we assume a triangulation of $\overline{\Omega_c}$ whose nodes coincide with lattice sites (will be referred to as nodal atoms) and compute the needed quantities: energy, forces, and stiffness matrix entries; the latter is required if we choose Newton-like methods for computing equilibrium of energy.

The atomistic contributions can be split into two groups, one involving only atoms in Ω_a and the rest:

$$E_a^{\text{acc}}(y) := \sum_{\substack{b \in \mathcal{B} \\ b \not\subset \Omega_c}} a_b(y) = \sum_{\substack{b \in \mathcal{B} \\ \bar{b} \subset \Omega_a}} a_b(y) + \sum_{\substack{b \in \mathcal{B} \\ \bar{b} \cap \Gamma \neq \emptyset}} a_b(y) =: E_{a,1}^{\text{acc}}(y) + E_{a,2}^{\text{acc}}(y). \quad (42)$$

The first sum is nothing but the standard sum of energies of bonds for atoms in Ω_a :

$$E_{a,1}^{\text{acc}}(y) = \sum_{\substack{(i,j) \in \mathcal{B} \\ i,j \in \Omega_a}} e_{(i,j)}(y) = \sum_{\substack{(i,j) \in \mathcal{B} \\ i,j \in \Omega_a}} \varphi(|y_j - y_i|).$$

The second sum in (42) requires extra care. In a general setting, one has to go through all the bonds, for each bond find all intersections with the interface Γ and compute the bond's contribution according to formula (39). According to Remark 2, the implementation can be simplified further if the atomistic region Ω_a is convex (or consists of convex disjoint sets), which is indeed the case for most of simulations of localized defects. In this case all bonds b such that $\bar{b} \cap \Gamma \neq \emptyset$ can be further

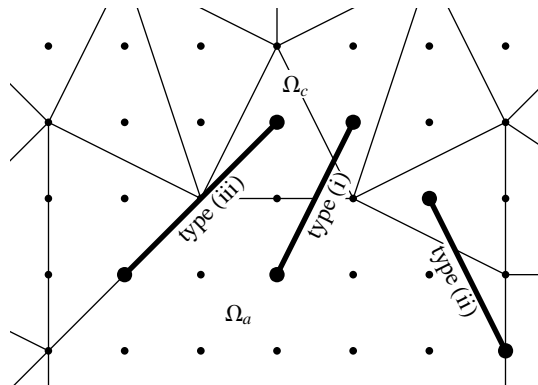


Figure 6: Illustration of three types of bonds that should be considered when implementing ACC for convex atomistic region Ω_a : (i) bonds that intersect Γ at one point, (ii) bonds that intersect Γ at two points, and (iii) bonds whose intersection with Γ is an interval.

categorized into: (i) bonds that intersect Γ at one point, (ii) bonds that intersect Γ at two points, and (iii) bonds whose intersection with Γ is an interval (see illustration on Figure 6).

For type (i) bonds, we find the point of intersection of a bond \bar{b} with the interface and compute the reconstruction of this point in terms of positions of nodal atoms on the interface. Using this reconstruction we can compute the corresponding contributions to energy, forces, and the stiffness matrix. The type (ii) bonds are treated in the same way, except that we need to compute reconstruction of both intersection points. The type (iii) bonds are treated similarly to type (ii) bonds: one should find reconstruction of two endpoint of intersecting interval and hence compute the contributions to energy, forces, and the stiffness matrix. According to formula (39), one has a factor of $w_m = 0.5$ for such bonds (since $\chi_{\Omega_c}|_{\Gamma} = 0.5$, cf. (38) and (29)). The list of coefficients of reconstruction can be precomputed once in the beginning of computation (and once per each mesh adaptation, if the latter is used). Then, at each iteration one has to go only through this list for assembling the contributions from bonds of type (i), (ii), and (iii).

4.6 Other Meshes

As a possible modification of the above methods, instead of requiring that the mesh nodes in the continuum region coincide with the lattice sites, we can require that the mesh nodes coincide with lattice half-sites (more precisely, the dual lattice sites), i.e., the nodes of mesh triangles T belong to the lattice $\mathbb{Z}^2 + (1/2, 1/2)$. One can follow the proof of Lemma 1 and show that in this case it is also possible to construct a triangle mT with m^2 copies of T reflected around integer points and shifted by integer vectors. Such a mesh is effectively used for those existing methods which assume that any atom fully belongs either to the atomistic region or the continuum region (i.e., that there are no atoms on the interface between the two regions).

5 Numerical Experiments

A number of numerical computations were conducted to illustrate the performance of the ACC method in 2D. The ACC method was implemented under the restriction that the atomistic/continuum interface is convex, as briefly described in Section 4.5. We first report the results of verification that the implemented ACC method indeed exhibits no ghost forces (Section 5.1) and then present the computations of a benchmark problem (Section 5.2).

A nonlinear conjugate gradient solver with linesearch [29] was used to find a stable equilibrium of an atomistic system. We used a simple Laplace preconditioner to accelerate convergence.

In all the numerical examples we used either the Lennard-Jones potential

$$\varphi(z) = -2z^{-6} + z^{-12}, \tag{43}$$

or the Morse potential

$$\varphi(z) = -2e^{\alpha(z-1)} + e^{2\alpha(z-1)}. \tag{44}$$

With these potentials the hexagonal lattice forms a stable equilibrium.

5.1 Verification of Zero Ghost Force

In this section we describe the computations conducted to verify that the proposed ACC method does not suffer from ghost forces.

We took a hexagonal atomic crystal as shown in Figure 7. The hexagon was centered at the origin, each side of the hexagon contained 129 atoms, and the total number of atoms in the system was 49537. The atomistic region formed a smaller hexagon also centered at the origin whose side contained K atoms, as illustrated in Figure 7(b) for $K = 8$. The atoms were interacting with the Lennard-Jones potential (43) with the cut-off distance R .

A series 80 tests, all with different values of $K = 1, 2, \dots, 10$, $R = 1.1, 3.1, 5.1, 7.1$, and the uniform deformation gradient $F = \begin{pmatrix} 1.01 & 0.01 \\ 0 & 1.01 \end{pmatrix}$, $\begin{pmatrix} 0.99 & 0 \\ 0.01 & 0.99 \end{pmatrix}$, was conducted. It was found that for all 80 tests the maximum force on the atoms in the atomistic region did not exceed 3.4×10^{-13} and the maximum generalized force on the finite element (FE) degrees of freedom did not exceed 4.7×10^{-12} , which are within the expected round-off error.

We further took the mesh from the previous example and randomly shifted its nodes (including the ones on the interface) by one or two lattice sites, as illustrated in Figure 8. We required the perturbation to yield the convex atomistic/continuum interface (this was a restriction for the implementation, but not the method). We conducted 100 random tests with $K = 10$, $R = 7.1$, $F = I$, and found that maxima of forces on atoms and FE degrees of freedom did not exceed 7.2×10^{-13} and 2.7×10^{-12} respectively, which are also within the expected round-off error.

Thus, the above results of numerical experiments with regular and distorted meshes in \mathbb{R}^2 numerically confirm that the proposed ACC method does not have ghost forces.

5.2 Comparison With Exact Solution

In this subsection we compare the results by the proposed ACC method (40) with the exact solution of atomistic equations. We also present the results by the straightforward coupling (8) (SF2) which was extended to 2D such that it does not have ghost forces for the nearest neighbor interaction.

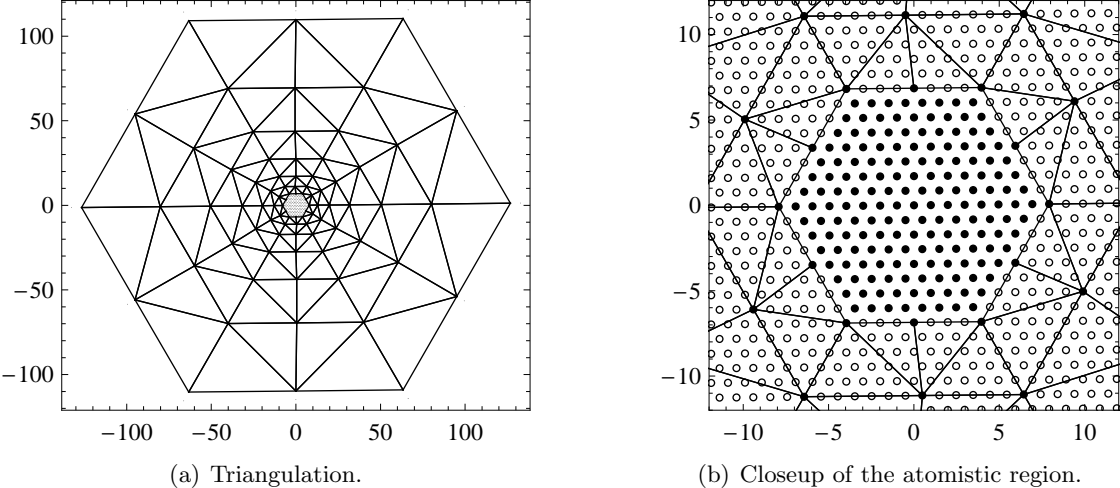


Figure 7: System of 49537 atoms forming a hexagon with the side of 129 atoms. Triangulation is shown on the left and the closeup of the atomistic region is shown on the right. In the right illustration, the atoms in the atomistic region as well as nodal atoms in the continuum region are bold. Illustration is for $K = 8$.

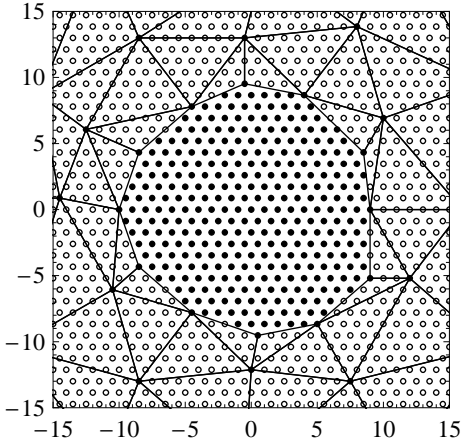


Figure 8: The same atomistic system as in Figure 7, but with randomly perturbed atomistic/continuum interface and triangulation nodes.

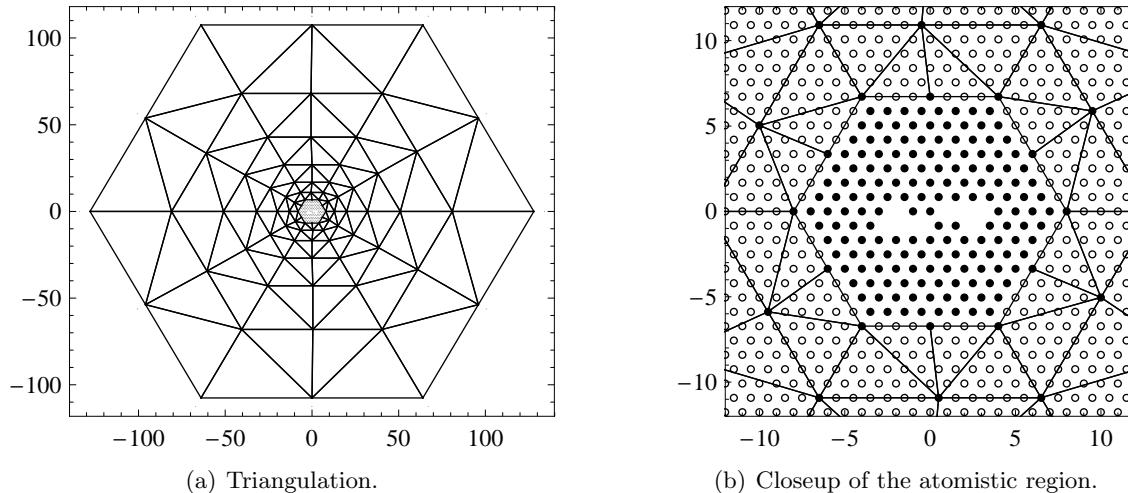


Figure 9: Reference configuration of the system of 49529 atoms forming a hexagon with the side of 129 atoms. Triangulation is shown on the left and the closeup of the atomistic region is shown on the right. Eight atoms has been removed to form a defect. Illustration is for $K = 8$.

The chosen benchmark problem was similar to the one in the previous subsection. The reference atomistic configuration is illustrated in Figure 9. We took a hexagonal atomic crystal, each side of the hexagon contains 129 atoms and the total number of atoms in the system is 49529. Eight atoms has been removed to form a defect in the center of the crystal. The atomistic regions formed a smaller hexagon also centered at the origin whose side contained K atoms, as illustrated in Figure 9(b) for $K = 8$.

Dirichlet-type boundary conditions were set: we extended the size of the hexagonal region by 3 and fixed the positions of the three added layers of atoms, so that every free atom in the system had the full set of neighbors to interact with; this is done in accordance with assumptions (26) and (27). The “external” deformation gradient $F = \begin{pmatrix} 1 & 0 \\ 0 & 0.97 \end{pmatrix}$ was applied to the positions of the added boundary atoms. Such an external compression forces atoms to occupy the empty lattice sites and form a defect, as illustrated in Figure 10.

There seem to be two stable equilibrium configurations associated with this test case. Therefore we first performed full atomistic computation to obtain one of the two stable equilibria, and then took it as an initial guess for the computations by the coupled methods.

Three tests were conducted: the first with the Lennard-Jones potential (Section 5.2.1), the second with a slowly decaying Morse potential (Section 5.2.2), and the third with the Lennard-Jones potential and perturbed atomistic/continuum interface (Section 5.2.3). The results of these computations are discussed in Section 6.

5.2.1 Test with Lennard-Jones Potential

In the first test case we let atoms interact with the Lennard-Jones potential (43) with the cut-off distance $R = 3.1$. We computed the solutions for $5 \leq K \leq 100$ with the two methods, ACC and

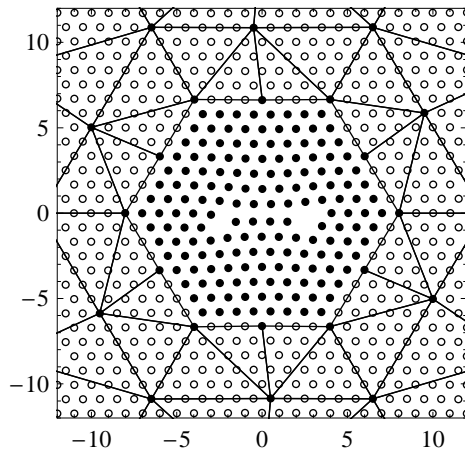


Figure 10: Computed deformation of the atomistic system, closeup of the atomistic region. A dislocation dipole defect can be seen. Computation is done with the ACC method for $K = 8$.

SF2, and calculated their errors. The errors were calculated as the difference between the respective coupled solution and the exact atomistic solution in the discrete $W^{1,\infty}$ -norm.

The discrete $W^{1,\infty}$ -norm of a deformation was defined as follows: for each triangle formed by the neighboring atoms in the reference configuration we compute the Jacobian of the mapping given by the deformations of those atoms, take the difference between the corresponding Jacobian of the exact solution and compute the matrix L^2 -norm of the difference. Taking maximum over all triangles of neighboring atoms yields the discrete $W^{1,\infty}$ -norm.

The results of computations are shown in Figure 11. We can see that the ACC method does converge whereas SF2 fails to converge due to ghost forces. The lowest error for the SF2 method was approximately 5×10^{-3} , which is acceptable in the engineering applications. The error of SF2 was small due to the second nearest neighbor interaction being relatively weak compared to the nearest neighbor interaction. In the next section we will see the results for the test case where the second nearest neighbor interaction is considerable.

5.2.2 Test with Slowly Decaying Morse Potential

In this test case we chose the Morse potential (44) with $\alpha = 3$ and the cut-off distance $R = 3.1$. The strength of such an interaction decays rather slowly and the ghost force effects should be more pronounced in this case. The external compression $F = \begin{pmatrix} 0.97 & 0 \\ 0 & 0.95 \end{pmatrix}$ was set as the boundary conditions. As before, the exact solution similar to the one shown in Figure 10 was taken as initial guess for the conjugate gradient iterations for the ACC and SF2 methods.

The results of computations are shown in Figure 12. As can be seen, for such a slowly decaying interaction the two methods produce rather different results. The error of the SF2 method stayed at the level of 0.07 no matter how large was the atomistic region. The error of the ACC method, in contrast, steadily decayed with increasing K and showed the behavior similar to the test case with the Lennard-Jones potential.

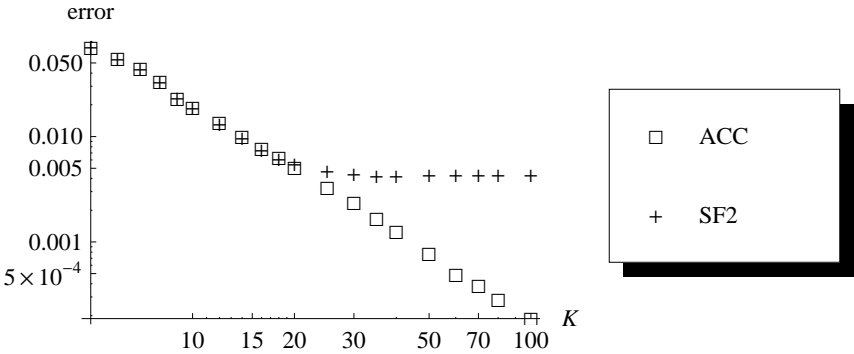


Figure 11: $W^{1,\infty}$ -errors of the computed solutions for the test with the Lennard-Jones potential. Computations were done by the two methods, ACC (defined in (40)) and SF2 (defined in (8)), for different sizes of the atomistic region ($5 \leq K \leq 100$), and compared with the exact atomistic solution. For small size of the atomistic region K , both methods show the same error. However with further increase of K , the ACC method shows steady convergence whereas SF2 fails to converge due to ghost forces.

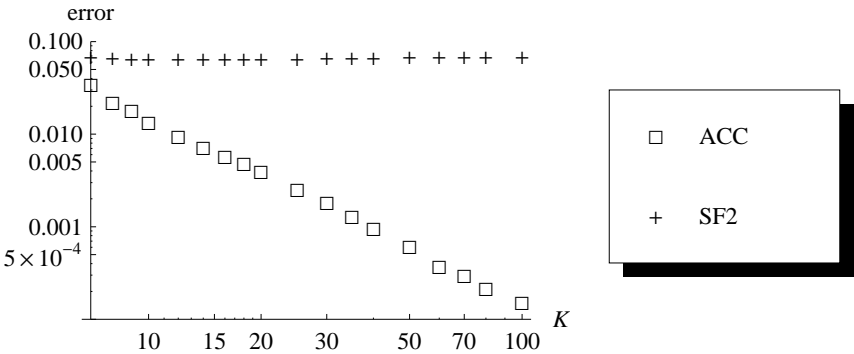


Figure 12: $W^{1,\infty}$ -errors of the computed solutions for the test with slowly-decaying Morse potential. Computations were done by the two methods, ACC (see (40)) and SF2 (see (8)), for different sizes of the atomistic region ($7 \leq K \leq 100$), and compared with the exact atomistic solution. The ACC method shows steady convergence as size of the atomistic region increases. In contrast, the error of the SF2 method is entirely dominated by the ghost force.

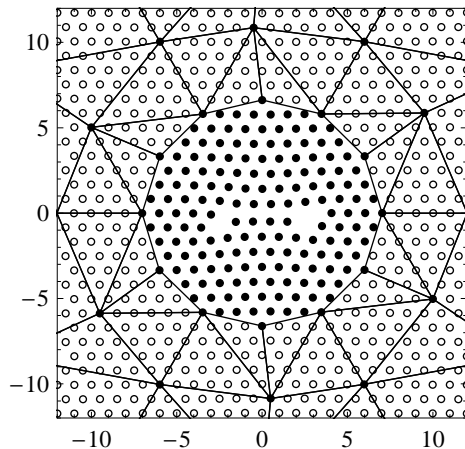


Figure 13: Atomistic/continuum interface of the test with non-aligned interface (atomistic domain size $K = 8$).

5.2.3 Test with Lennard-Jones Potential and Non-Aligned Interface

The last test case is similar to the first one (Section 5.2.1), except that we perturbed the nodes of the atomistic/continuum interface: namely, we shifted the corner of the interface by one lattice site towards the center (see Figure 13).

The results of computations are shown in Figure 12. Surprisingly, the perturbation of the interface essentially did not affect the error of ACC, but drastically changed the behavior of SF2. First, we see that the smallest error of SF2 is 0.03, compared to 5×10^{-3} in the aligned interface case. Second, the error of SF2 showed increase up to 0.1 when the atomistic region size was $K = 50$. Such large errors are normally not acceptable in the applications.

6 Discussion

The main observation that can be made from the results of computations is that the proposed ACC method exhibits steady convergence as the atomistic domain size is increased, and is not sensitive to whether the nearest neighbor interaction dominate or whether the atomistic/continuum interface is aligned with the lattice. This is in contrast with the results by the straightforward coupling (SF2), which formally does not converge. In favorable circumstances, the error of SF2 was within the commonly acceptable limit, but was found to be considerably large for a slowly decaying interaction or a non-aligned interface.

Particularly, it was found that if we distort the interface, the error of the ACC method remained quantitatively the same as for the undistorted interface (compare the squares and the dashed line in Figure 14). This finding is important for the practical applications, where the mesh is refined according to solution gradients. For the present method it is not required to align the mesh along the crystalline lattice or to fully refine it near the atomistic/continuum interface.

The ACC method proposed and tested in the present work couples the atomistic and continuum degrees of freedom only through the interface, which offers some convenience for implemen-

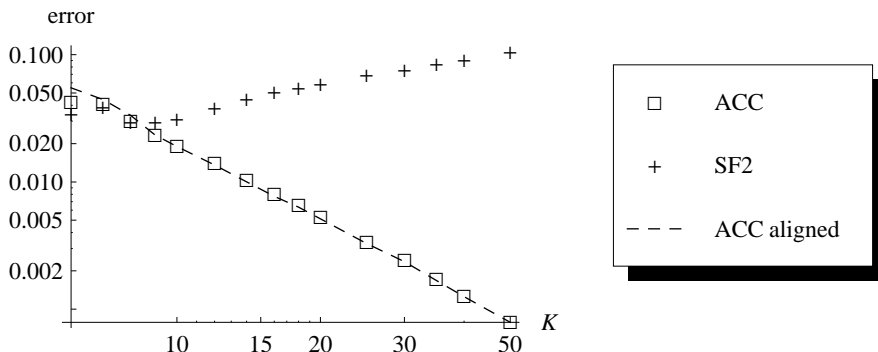


Figure 14: $W^{1,\infty}$ -errors of the computed solutions for the test with the Lennard-Jones potential and non-aligned interface: $W^{1,\infty}$ -errors of the computed solutions. Computations were done by the two methods, ACC (see (40)) and SF2 (see (8)), for different sizes of the atomistic region ($6 \leq K \leq 50$), and compared with the exact atomistic solution. The dashed line is the error of ACC for the test with the aligned interface (Section 5.2.1). The ACC method shows steady convergence as size of the atomistic region K increases from 7 to 50 and is seen to be unaffected by the perturbation of the interface. On the contrary, the error of the SF2 method is much larger than for the aligned interface case, and grows as K increases.

tation. The coupling can be formulated in terms of reconstruction of position of points on the atomistic/continuum interface (as outlined in Section 4.5). The reconstruction coefficients can be precomputed, which will optimize the performance of the method.

The present method can be used in conjunction with the projection method described in [22] in which it is proposed to apply finite element interpolation directly in some parts of the atomistic region. One could design a method with a transitional atomistic region where the piecewise affine finite elements are used, but the exact atomistic energy is computed. Such a hybrid method will also be free from ghost forces.

In the present paper, we assumed that the partition of the crystal in atomistic and continuum regions and the mesh in the continuum region are given. In practice, a good choice of the regions and the mesh are often not known a priori and one has to rely on algorithms to adaptively determine them. The purely energy-based formulation of the proposed method may help in designing adaptive algorithms based on rigorous a posteriori error estimates, similar to the ones in finite elements [34]. Such algorithms have been proposed and tested in 1D [1, 27].

There are two main challenges that need to be addressed for the present method to become competitive with existing methods on majority of realistic engineering problems. The first challenge is extension of the proposed methods to 3D problems. In three dimensions it is not yet clear how the continuum energy can be split into contributions defined as line integrals, as follows from Remark 1.

The other major challenge is formulation of the method for many-body potentials, as the two-body potentials are far from covering all the existing atomistic models. In this regard, we should note that there exists a method of atomistic/continuum coupling (namely, the geometrically consistent scheme of E, Lu, and Yang [13]) which is free from ghost forces under the restriction of

planar aligned interface with no corners, but for general potentials. This indicates that the present method could also be extended to general potentials.

It would also be interesting to extend the present method to coupling of atomistic model with non-discretized continuum model in many dimensions. In that case one can discretize the continuum model with higher degree polynomials and obtain an increased accuracy of the overall method. Another extension which would be useful for applications is to formulate the proposed method for complex lattices, in which case the method will be applicable, for instance, to those alloys which are described by two-body potentials (for an example of such 2D model see [16]).

Acknowledgment

The author is indebted to Christoph Ortner for motivating discussions during the OxMOS/MD-network workshop, and for many valuable comments on the manuscript.

7 Conclusion

We considered the problem of consistent coupling of atomistic and continuum models of materials, limited to the case of 1D or 2D zero-temperature statics. We proposed two versions of energy-based coupling which are consistent (i.e., do not suffer from interfacial errors) by construction. The coupling is based on judiciously defining the contributions of the atomistic bonds to the discrete and the continuum potential energies; the same coupling in 1D has been independently proposed and analyzed in [21]. The proposed energy-based coupling is limited to a two-body potential and one or two spatial dimensions; extending it to general potentials and 3D is left for future developments.

References

- [1] M. ARNDT AND M. LUSKIN, *Goal-oriented adaptive mesh refinement for the quasicontinuum approximation of a Frenkel-Kontorova model*, *Comput. Methods Appl. Mech. Engrg.*, 197 (2008), pp. 4298–4306.
- [2] M. BORN AND K. HUANG, *Dynamical Theory of Crystal Lattices*, Oxford University Press, 1954.
- [3] J. Q. BROUGHTON, F. F. ABRAHAM, N. BERNSTEIN, AND E. KAXIRAS, *Concurrent coupling of length scales: Methodology and application*, *Phys. Rev. B*, 60 (1999), pp. 2391–2403.
- [4] W. A. CURTIN AND R. E. MILLER, *Atomistic/continuum coupling in computational materials science*, *Modelling Simul. Mater. Sci. Eng.*, 11 (2003), pp. R33–R68.
- [5] M. DOBSON AND M. LUSKIN, *Analysis of a force-based quasicontinuum approximation*, *Math. Model. Numer. Anal.*, 42 (2008), pp. 113–139.
- [6] ———, *Iterative solution of the quasicontinuum equilibrium equations with continuation*, *J. Sci. Comput.*, 37 (2008), pp. 19–41.
- [7] ———, *An optimal order error analysis of the one-dimensional quasicontinuum approximation*, *SIAM. J. Numer. Anal.*, 47 (2009), pp. 2455–2475.

- [8] M. DOBSON, M. LUSKIN, AND C. ORTNER, *Accuracy of quasicontinuum approximations near instabilities*, 2009. arXiv.org:0905.2914.
- [9] —, *Iterative methods for the force-based quasicontinuum approximation*, 2009. arXiv.org:0910.2013.
- [10] —, *Sharp stability estimates for force-based quasicontinuum methods*, *Multiscale Model. Simul.*, 8 (2010), pp. 782–802.
- [11] —, *Stability, instability, and error of the force-based quasicontinuum approximation*, *Arch. Ration. Mech. Anal.*, (to appear). arXiv:0903.0610.
- [12] M. DOBSON, C. ORTNER, AND A. V. SHAPEEV, *The spectrum of the force-based quasicontinuum operator for a periodic chain*, 2010. In review (preprint version: arXiv:1004.3435).
- [13] W. E, J. LU, AND J. Z. YANG, *Uniform accuracy of the quasicontinuum method*, *Phys. Rev. B*, 74 (2006), pp. 214115(1–12).
- [14] B. EIDEL AND A. STUKOWSKI, *A variational formulation of the quasicontinuum method based on energy sampling in clusters*, *J. Mech. Phys. Solids*, 57 (2009), pp. 87–108.
- [15] J. FISH, M. A. NUGGEHALLY, M. S. SHEPHARD, C. R. PICU, S. BADIA, M. L. PARKS, AND M. GUNZBURGER, *Concurrent AtC coupling based on a blend of the continuum stress and the atomistic force*, *Comput. Methods Appl. Mech. Engrg.*, 196 (2007), pp. 4548–4560.
- [16] O. KASTNER, *Molecular-dynamics of a 2d model of the shape memory effect - part i: Model and simulations*, *Contin. Mech. Thermodyn.*, 15 (2003), pp. 487–502.
- [17] P. A. KLEIN AND J. A. ZIMMERMAN, *Coupled atomistic-continuum simulations using arbitrary overlapping domains*, *J. Comput. Phys.*, 213 (2006), pp. 86–116.
- [18] J. KNAP AND M. ORTIZ, *An analysis of the quasicontinuum method*, *J. Mech. Phys. Solids*, 49 (2001), pp. 1899–1923.
- [19] S. KOHLHOFF AND S. SCHMAUDER, *A new method for coupled elastic-atomistic modelling*, in *Atomistic Simulation of Materials: Beyond Pair Potentials*, V. Vitek and D. J. Srolovitz, eds., Plenum Press, New York, 1989, pp. 411–418.
- [20] F. LEGOLL, *Multiscale methods coupling atomistic and continuum mechanics: some examples of mathematical analysis*, in *Analytical and numerical aspects of partial differential equations*, Walter de Gruyter, Berlin, 2009, pp. 193–245.
- [21] X. H. LI AND M. LUSKIN, *A generalized quasi-nonlocal atomistic-to-continuum coupling method with finite range interaction*, 2010. manuscript (preprint version: arXiv:1007.2336).
- [22] P. LIN AND A. V. SHAPEEV, *Energy-based ghost force removing techniques for the quasicontinuum method*. In review (preprint version: arXiv:0909.5437).
- [23] B. Q. LUAN, S. HYUN, J. F. MOLINARI, N. BERNSTEIN, AND M. O. ROBBINS, *Multiscale modeling of two-dimensional contacts*, *Phys. Rev. E*, 74 (2006), p. 046710.

- [24] R. E. MILLER AND E. B. TADMOR, *A unified framework and performance benchmark of fourteen multiscale atomistic/continuum coupling methods*, Modelling and Simulation In Materials Science and Engineering, 17 (2009), p. 053001.
- [25] P. B. MING AND J. Z. YANG, *Analysis of a one-dimensional nonlocal quasi-continuum method*, Multiscale Model. Simul., 7 (2009), pp. 1838–1875.
- [26] C. ORTNER, *A priori and a posteriori analysis of the quasi-nonlocal quasicontinuum method in 1D*. arXiv:0911.0671, 2010.
- [27] C. ORTNER AND E. SÜLI, *Analysis of a quasicontinuum method in one dimension*, M2AN Math. Model. Numer. Anal., 42 (2008), pp. 57–91.
- [28] V. B. SHENOY, R. MILLER, E. B. TADMOR, D. RODNEY, R. PHILLIPS, AND M. ORTIZ, *An adaptive finite element approach to atomic scale mechanics — the quasicontinuum method*, J. Mech. Phys. Solids, 47 (1999), pp. 611–642.
- [29] J. R. SHEWCHUK, *An introduction to the conjugate gradient method without the agonizing pain*, 1994. Available from <http://www.cs.cmu.edu/~quake-papers/painless-conjugate-gradient.pdf>.
- [30] L. E. SHILKROT, R. E. MILLER, AND W. A. CURTIN, *Coupled atomistic and discrete dislocation plasticity*, Phys. Rev. Lett., 89 (2002), p. 025501.
- [31] T. SHIMOKAWA, J. J. MORTENSEN, J. SCHIØTZ, AND K. W. JACOBSEN, *Matching conditions in the quasicontinuum method: Removal of the error introduced at the interface between the coarse-grained and fully atomistic region*, Phys. Rev. B, 69 (2004), pp. 214104(1–10).
- [32] W. G. STRANG AND G. J. FIX, *An analysis of the finite element method*, Wellesley Cambridge Pr, 1973.
- [33] E. B. TADMOR, M. ORTIZ, AND R. PHILLIPS, *Quasicontinuum analysis of defects in solids*, Philosophical Magazine A, 73 (1996), pp. 1529–1563.
- [34] R. VERFÜRTH, *A review of a posteriori error estimation and adaptive mesh-refinement techniques*, Wiley-Teubner, Amsterdam, 1996.
- [35] G. J. WAGNER AND W. K. LIU, *Coupling of atomistic and continuum simulations using a bridging scale decomposition*, J. Comput. Phys., 190 (2003), pp. 249–274.
- [36] S. P. XIAO AND T. BELYTSCHKO, *A bridging domain method for coupling continua with molecular dynamics*, Comput. Methods Appl. Mech. Engrg., 193 (2004), pp. 1645–1669.